Journal of Sound and Vibration (1998) **214**(5), 805–815
Article No. sv981551

VIBRATION ANALYSIS OF ROTATING MACHINERY USING THE SPECTRAL DISTRIBUTION FUNCTION

S. S. Davis
Fluid Mechanics Laboratory, *NASA Ames Research Center*, *Moffett Field CA* 94035, *U.S.A.*

(*Received* 19 *May* 1997, *and in final form* 3 *February* 1998)

The spectral distribution function is used to characterize the vibration signal of rotating machinery. It is shown to be a more robust indicator than conventional power spectral density estimates, but requires only slightly more computational effort. The method is demonstrated with a model of a defective bearing. The spectral distribution function is applied to practical problems involving seeded helicopter transmission faults and the vibration signal from a ground-based vacuum compressor system.

1. INTRODUCTION

Vibration waveforms are information-rich signals that must be carefully examined in order to identify evolving faults in rotating machinery. Typically, algorithms may include code for specific microscopic defects or may be general indicators of overall machinery health. In either case, effective signal characterization is of primary importance. In the latter case, a simple examination of the data stream would report peak amplitudes (displacement, velocity, or acceleration) over long time periods with basic feature extraction using alarms triggered by excursions beyond pre-selected limits. This approach has a long history and is clearly the appropriate procedure in many cases. Strip chart recording technology (or its digital counterpart) is all that is needed to realize this diagnostic level. Data trending using simple statistical methods can indicate needed maintenance and extrapolation of these data to future times can even serve as a predictor of failure. The next level of complexity is to explore the distribution of vibrational energy over a frequency range using spectrum analysis tools. Even with crude analog instrumentation, spectral information is a powerful tool in the hands of experienced users. These tools were not always available to users in the field who needed this data for day-to-day decision making. Digital fast Fourier transform methods (FFTs) were recently made available to a wide user community and are now being used in many applications that previously depended on simpler statistics such as peak-to-peak or RMS readings.

In a related development, tools to interpret and recognize specific patterns residing in the large quantity of digital data being generated are just now being introduced. Much of this work is still in the research phase and new approaches using short-time analysis of vibration records are under active investigation [1–3]. An important step to improve the data trending algorithms now in use is to consider the time-evolution of the spectral information. This process involves using short-time spectral data to assess long-time health of the equipment.

0022–460X/98/300805 + 11 $30.00/0

A conventional display of the spectra in the two-dimensional time-frequency domain is the ''waterfall plot'' generated by commercial vibration monitoring systems. This name derives from the manner in which these plots are generated by stacking conventional short time amplitude or power spectra over a longer time interval. A problem with this type of display is that random noise is revealed as erratic hills and valleys which are difficult to reconcile in the time direction. Also, due to certain peculiarities associated with digital Fourier analysis, it may be difficult to discern specific events from the background signal. These waterfall plots usually serve as qualitative diagnostic tools.

In this paper a new approach is presented to quantify a vibration signature in the frequency–time domain. It is based on representing certain aspects of the spectral distribution function (SDF) as it evolves in frequency–time space. The SDF is a derivation of the power spectral density (PSD). It bears the same relation to the PSD as a probability distribution function does to a probability density function. This method has the significant advantage of being able to characterize the long-time behavior of high bandwidth mixed signals with a small number of parameters. In a sense, it is an approach to data compression and may be a useful tool for applying image processing and machine learning concepts.

The plan of this paper is to first present the method using simple illustrative examples. The SDF is first applied to a hypothetical bearing vibration problem. It is then applied to actual gearbox vibration data from a helicopter drive train to illustrate the effect of gear tooth defects on the SDF. Finally, the procedure is applied to the vibration signal from a ground-based centrifugal compressor during normal day-to-day operation.

2. THE SPECTRAL DISTRIBUTION FUNCTION

Spectral analysis is probably the most widely used tool to describe vibration signals. However, raw spectra in the presence of noise behave erratically and its message is not always easy to interpret. Procedures to smooth raw spectra have been developed over the years. The two major approaches are direct calculation of ensemble averaged PSDs and parametric methods using time series models [4]. Another approach is to smooth an estimated PSD by partial integration and this is the basis for the SDF.

This subject can be approached from many directions. Here the process will be treated from the point of view of statistical time series analysis. It was shown by Wold in 1938 (as cited in reference [5]) that there exists a *monotonically increasing bounded function* $F(\omega)$ defined in the interval $-\pi < \omega < \pi$ such that

$$R(k) = \int_{-\pi}^{\pi} \mathrm{e}^{\mathrm{i}k\omega}\, \mathrm{d}F(\omega) = \int_{-\pi}^{\pi} \mathrm{e}^{\mathrm{i}k\omega} S(\omega)\, \mathrm{d}\omega, \tag{1}$$

where $R(k)$ is a stationary auto covariance function of a time series with lag k. The function $F(\omega)$ is the spectral distribution function (SDF). It has the following properties: (1) it is an integrable non-negative function; (2) it has a finite number of discontinuities; (3) it has a continuous part that is differentiable.

If the SDF contains only discontinuities and is otherwise flat, the underlying signal has a discrete spectrum; if only the continuous part exists is it a continuous function. The slope of $F(\omega)$ is the PSD $S(\omega)$, but is only rigorously defined for continuous spectra. An approximation to the power spectral density (or its amplitude equivalent) is the conventional output of vibration analyzers.

A more practical approach to the SDF is to define a PSD estimate from its periodogram representation. An N point time series X_j sampled at Δt is transformed as:

$$C_k = \sum_{j=1}^{N} X_j \, e^{2\pi i (j-1)(k-1)/N}, \qquad k = 1, \ldots, N. \tag{2}$$

The periodogram at $M = N/2 + 1$ points is defined by

$$S_1 = S(f_1)\,(1/N^2) C_1 C_1^*, \quad S_k = S(f_k) = (1/N^2)\,(C_k C_k^* + C_{N+2-k} C_{N+2-k}^*), \quad k = 2, M-1,$$
$$S_M = S(f_M) = (1/N^2) C_M C_M^*, \tag{3}$$

where an asterisk indicates the complex conjugate. This is an M-line estimate at the frequencies $f_k = (k-1)/(N\Delta t)$. The periodogram is defined so that its sum is equal to the mean squared amplitude, a measure of the total signal energy. The SDF estimate is simply the partial summation

$$F_k = \sum_{j=1}^{k} S_j, \tag{4}$$

where k varies from 1 to M. In particular, the last value F_M is the mean square amplitude.

From its definition $F_k = F(f_k)$ is the proportion of energy at and below the indicated frequency. In some applications the SDF can be normalized by its last and maximum value and the normalized spectral distribution function (NSD) measures the fraction of mean square energy at and up to any frequency. It must be emphasized that manipulating the power spectral density does not add or subtract information; it is just a convenient smoothing process for further analysis and interpretation. All the quantities considered are estimates of the second-order statistical moments, an important characteristic of the underlying physical process.

3. EXAMPLES OF THE SPECTRAL DISTRIBUTION FUNCTION

Gaussian white noise is generated at $N = 500$ points. This zero-mean, finite-length, stationary time series has a 251 line periodogram as defined by equation (3). The estimated PSD has a mean square amplitude of 0·993 and is shown in Figure 1(a). The theoretical (uniform) power spectral density for the Gaussian white noise process is 0·00397 and is also indicated in the figure. The data shown in Figure 1(a) is further processed using equation (4) to generate the SDF. This is shown in Figure 1(b) with the corresponding

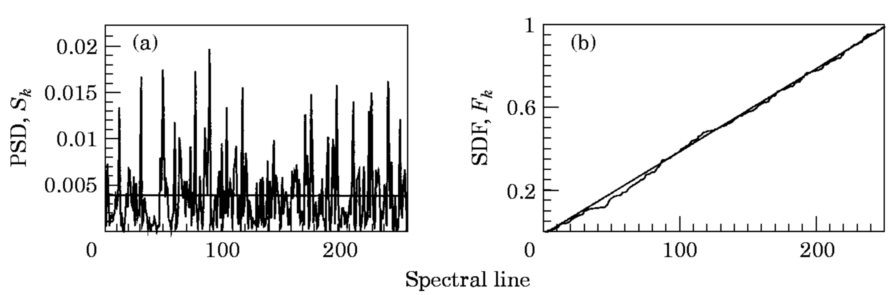

Figure 1. (a) Power spectral density (PSD) estimate for Gaussian white noise. $N = 500$ points, $M = 251$ spectral lines. (b) Spectral distribution function (SDF) for the Gaussian white noise process derived from the PSD. Theoretical PSD and SDF shown by straight lines.

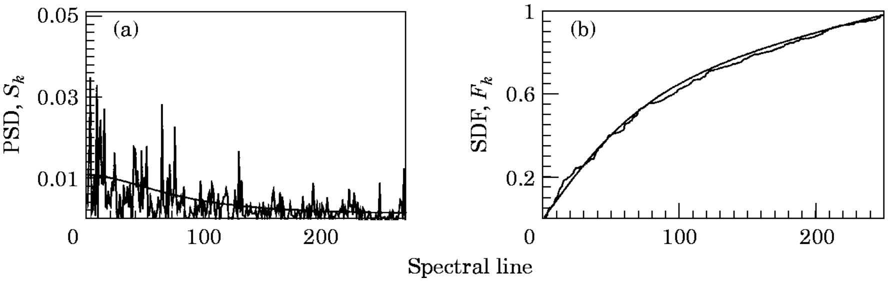

Figure 2. (a) Power spectral density estimate for a modified random walk process $X_n = \alpha X_{n-1} + G_n$, $\alpha = 0{\cdot}4$. $N = 500$ points. (b) Spectral distribution function for the random walk process. Theoretical values shown by smooth solid curves.

theoretical curve which is now a line of constant slope. The partial summation process defining the distribution function smoothes the data and, by appearance at least, seems to generate a more pleasing representation of Gaussian white noise. A practical application of the SDF for random noise processes was proposed in 1955 by Bartlett (cited on p. 54 of reference [4]) who suggested representing sample data in this format and measuring its deviation from the theoretical straight line as an indication of the spectral uniformity of the data.

The next sequence examines a process with a shaped spectrum. It is taken from a modified random walk model defined by the recurrence relation $X_n = \alpha X_{n-1} + G_n$, where X_n is a time series, G_n is the aforementioned Gaussian process, and α a parameter. The exact time series is given by the particular solution of the first order non-homogeneous difference equation [6]. It is

$$X_n = \textstyle\sum_{j=1}^{n} G_j\, \alpha^{n-j}$$

which is only stable for $-1 < \alpha < 1$. The auto covariance function, expressed in terms of the lag k, is $R(k) = \alpha^k/(1-\alpha^2)$. The theoretical continuous spectral density of the discrete auto covariance function from equation (1) is

$$S(\omega) = \frac{1}{1-\alpha^2}\sum_{k=-\infty}^{k=\infty} \alpha^k\, \mathrm{e}^{-\mathrm{i}k\omega} = \frac{1}{1-\alpha^2}\left(1 + 2\sum_{k=1}^{k=\infty} \alpha^k \cos(k\omega)\right). \tag{5}$$

This one-sided spectrum is continuous in the range $0 < \omega < \pi$. The exact continuous power spectral density and spectral distribution function are obtained from the summation of equation (5) and an indefinite integration:

$$S(\omega) = 1/(1 - 2\alpha\cos(\omega) + \alpha^2), \qquad F(\omega) = 2\tan^{-1}([1+\alpha]/[1-\alpha]\tan(\omega/2)). \tag{6a, b}$$

A 500 point time series version of the random walk model is processed to obtain a periodogram representation as described above. The estimated PSD is shown in Figure 2(a) along with the theoretical values from equation (6a). (The variable $\omega = \pi$ is scaled to the last spectral line $M = 251$.) The spectrum decreases monotonically, but this behavior is only vaguely hinted at by the PSD estimate. The corresponding spectral distributions are displayed in Figure 2(b) where the theoretical estimate was normalized so they both match at the last spectral line. The SDF shows clearly the rapid energy rise and subsequent slower increase to its final energy state. This is a much better parameter with which to gauge the distribution of energy. A simple index of the energy distribution is the frequency at a given ordinate. For example, approximately 80% of the energy resides at frequencies at and below spectral line 150. These examples are quite straightforward when applied to continuous spectra, but most practical problems in vibration analysis are dominated by discrete frequencies. These cases will be considered next.

4. A HYPOTHETICAL VIBRATION PROBLEM

The evolution of certain features of the spectral distribution function is illustrated with a hypothetical rotating machinery example. The particular case considered is a simplified model of ball-bearing wear [7]. Bearing defects evolve over time and appear in the vibration signature as a number of discrete modes whose amplitude and frequency vary slowly in time. Simple statistical measures such as records of short time r.m.s. values may not capture these events. To be specific, let a fictitious bearing possess baseline vibrations at non-integer related frequencies of 570 and 875 Hz. A short burst of 500 data points are sampled at 10 000 Hz (total record length = 50 ms) and passed through a standard spectrum analyzer without windowing or other pre-processing to obtain a periodogram. The vibration frequency and amplitude changes on a time scale measured in hours. The amplitude changes at each frequency are artificially adjusted so that the RMS value always remains constant. (Thus, an r.m.s. record would show no changes with time.)

Initial and final power spectral densities and spectral distribution functions are shown in Figure 3 for the case when the upper frequency changes from 875 to 1050 Hz over an eight hour period. The amplitude of the signal is fixed at 2 for each of the two frequencies and the mean square amplitude is 4. Note that the PSD peaks are not reliable indicators (each peak in Figure 3(a) should have a value of 2) due to leakage of the spectral information to neighboring frequencies. However, the initial-time SDF in Figure 3(b) behaves as a step function and jumps to the appropriate values of 2 and 4. It represents a true indicator of the energy partition between the two frequencies. (Leakage is reflected in the SDF by a slight broadening of the steps.). The periodogram in Figure 3(c) represents the case when the amplitudes have changed to 2·58 and 1·17 respectively and the upper

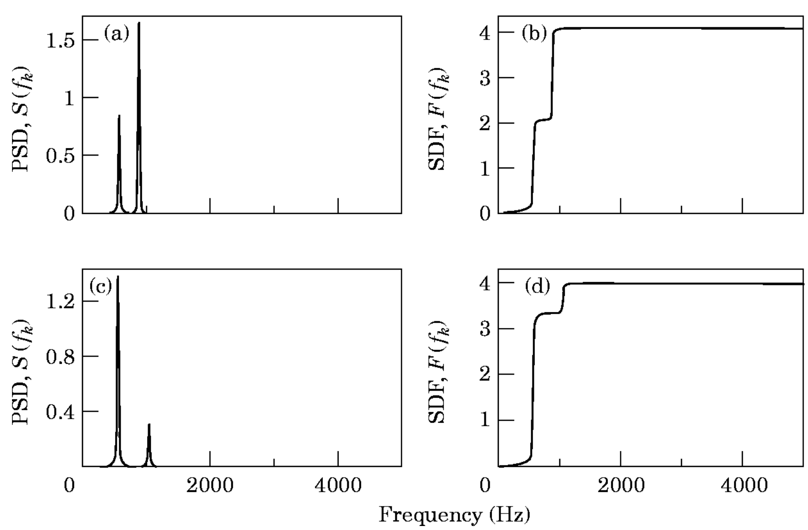

Figure 3. PSD and SDF functions for a bearing model. (a) 500-point PSD for signals at 570 and 875 Hz sampled at 10 000 Hz. The amplitude of each signal is 2. (b) SDF derived from the PSD in (a). (c) PSD for signal after 8 hr when upper frequency has increased by 20% and amplitudes have changed to 2·58 and 1·17 respectively. (d) SDF corresponding to (c).

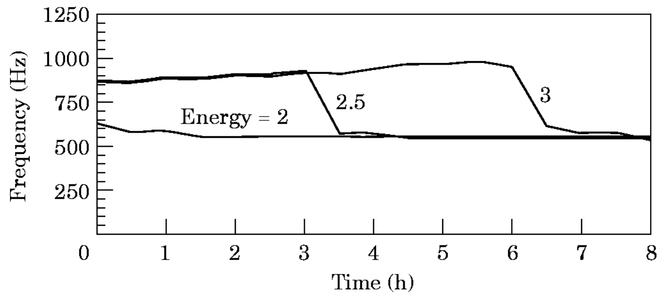

Figure 4. Frequency-time diagram illustrating how SDF contours can be used to indicate changes in vibration signals.

frequency has increased by 20% to 1050 Hz. The final-time energy partition is shown in Figure 3(d) and has unequal steps while the final mean square amplitude is unchanged.

A representation in the frequency–time plane of the contours at energy levels 2, 2·5, and 3 are shown in Figure 4. The slow frequency drift is easily discernible by the slope of the higher frequency while the lower frequency remains constant. Since the energy partition varies with time, at some point the energy = 2·5 contour cascades to the lower frequency. This occurs soon after 3 hr; the energy = 3 contour drops at a later time. The lowest contour remains at the baseline frequency. These contours are simple and self-consistent enough to relate these "symptoms" to any underlying "disease." In a practical situation data reflecting nominal operating conditions must be recorded and archived to serve as a baseline.

As mentioned many times in the literature, spectral estimates are very difficult to interpret in some cases since the energy at arbitrary discrete frequencies are dissipated due to leakage effect. This is because frequencies occur that are not integer orders of the basic sampling rate and conventional spectra can be misleading. The current representation of the evolutive process in terms of the SDF as in Figures 3(b) and 3(d) are more consistent measures.

5. HELICOPTER GEARBOX DATASET

The next example is from a seeded fault in an actual helicopter gearbox. Vibration data was measured on a helicopter tail rotor drive train gearbox [8]. Specific faults were "seeded" in the gear train and the vibration signatures recorded using accelerometer sensors. Data was first recorded on magnetic tape and then digitized and phase averaged with respect to the shaft rotation. Published data was recorded at a sample rate of 46 880 Hz using a total of N = 46 880 points giving a real time record length of 1 s. There are approximately 650 data samples per shaft revolution.

Three data sets from this test series are examined: (1) the baseline data set with no seeded faults, (2) data seeded with gear spalls on two teeth, and (3) data obtained with half of one gear tooth removed. The power spectral density (in dB) for the baseline case is shown in Figure 5(a). The spectrum is fairly typical of this type with a few tones appearing above the background noise. The spectral distribution function normalized by its maximum value (the mean square amplitude) is denoted by NSD and is shown in Figure 5(b). Discrete jumps indicate the tones and rising slopes denote the build up of frequency-dependent continuous random noise. The contribution of the tone at about 2000 Hz is very visible in the figure. (This tone would appear more prominently if the power spectral density were plotted on a linear scale.) The quantifiable indicators in the NSD are the frequencies that bound certain energy levels. For example, the first and last deciles are indicated by dashed lines in the figure. Corresponding data for the seeded faults are shown in Figures 6 and 7. There are definite changes in the power spectra, but the changes in the NSD are much more obvious and easily quantifiable. The 10% and 90% deciles are also indicated and

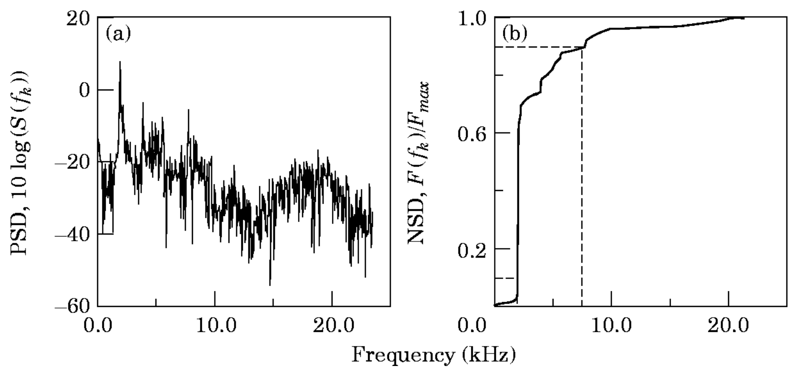

Figure 5. (a) Power spectral density from an accelerometer mounted on a helicopter gearbox. Test Case 1: baseline data. (b) Normalized spectral distribution for Test Case 1, decile values at 10% and 90% as noted.

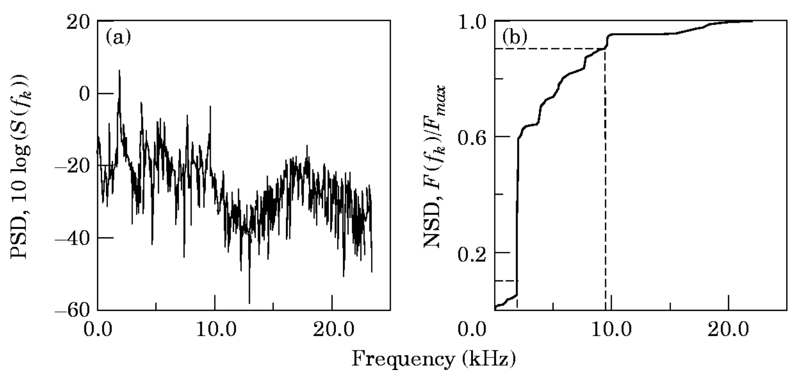

Figure 6. (a) Power spectral density from an accelerometer mounted on a helicopter gearbox. Test Case 2: seeded spalls on gear. (b) Normalized spectral distribution for Test Case 2, decile values at 10% and 90% as noted.

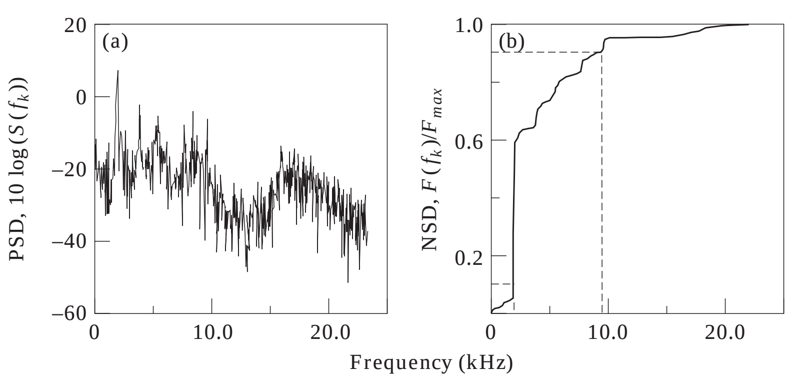

Figure 7. (a) Power spectral density from an accelerometer mounted on a helicopter gearbox. Test Case 3: seeded gear defect with tooth removed. (b) Normalized spectral distribution for Test Case 3, decile values at 10% and 90% as noted.

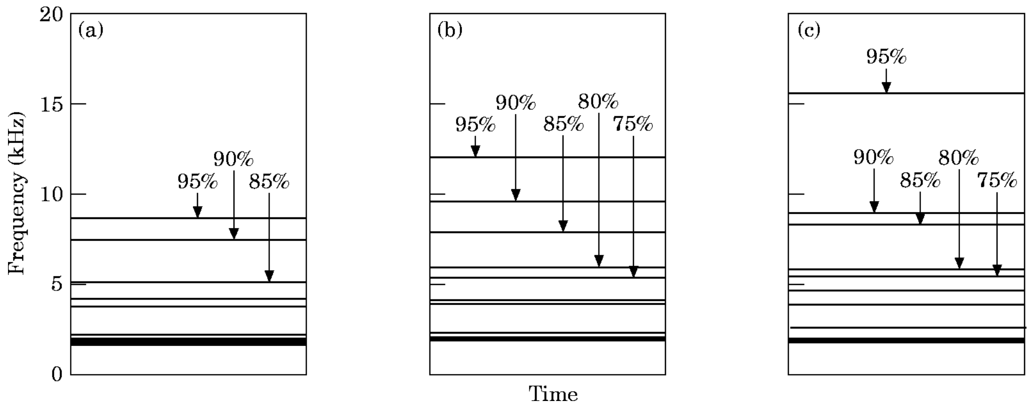

Figure 8. Contour plot representation of helicopter gearbox data sets. Lines define maximal frequencies bounding the indicated percentage of mean square energy. (a) Baseline (no faults), (b) data set 2 (spalling), (c) data set 3 (tooth removed).

are different for each case. The normalized spectral distributions also show the apportionment of the mean square energy among discrete and continuous modes. In this case, a large amount (about 80%) of the energy resides in discrete tones.

A more meaningful way to present the data is to generate contour plots in the time-frequency domain. In Figure 8 all three cases are shown as contours of constant values of the normalized spectral distribution function at 5% increments. Changing contour levels reflect the effect of the seeded faults. These contours do not reflect only high frequencies, but are cumulative indicators of all frequencies below those indicated. Such features are easily captured and quantified using computer imaging techniques and point the way to possible automated analysis. Of course, gearbox vibration signals are notoriously complex and each installation has unique characteristics. More analysis needs

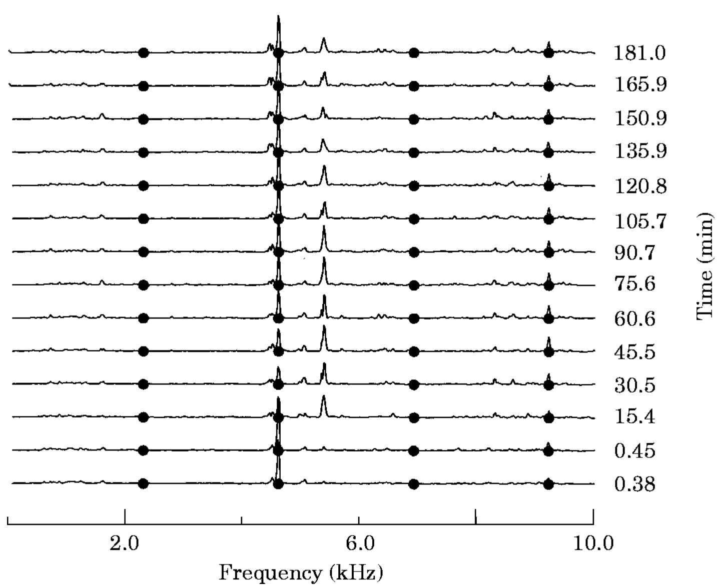

Figure 9. Cascade plot of vibration power spectra for a ground-based compressor. The accelerometer is located on the input shaft of a 1·71:1 ratio speed increaser. The elapsed time shown on right and solid symbols denote the first four gear mesh frequencies.

to be done on particular configurations in order to effectively monitor this class of equipment.

6. CENTRIFUGAL COMPRESSOR DATASET

The last example shows vibration data from a ground-based air compressor system. The compressor is used as a vacuum source for fluid mechanics experiments and can draw up to 240 000 c.f.m. It drives up to four indraft research wind tunnels in serial or parallel modes. The vacuum system consists of an 8000 Hp motor, a speed increaser, and a centrifugal vacuum pump. Accelerometers were installed at strategic locations on the input and output shafts of the speed increaser. The basic gear meshing frequency of the helical-geared speed increaser is 2300 Hz under nominal operating conditions with the input shaft rotating at 1790 r.p.m. The speed increaser's bull and pinion gears have 77 and 45 teeth respectively. A commercially available turbine-vibration monitoring system was used to process the accelerometer signal. The vibration monitoring system presents a 501-line PSD at 20 Hz intervals to an upper frequency of 10 kHz. Figure 9 shows a cascade plot of the short-time PSD at 14 discrete times during the approximately 3 hr of continuous operation. (The transient start-up and shut-down sequences are not shown.) The accelerometer whose data is shown in Figure 9 was located at the input of the speed increaser and measures horizontal acceleration. As indicated in the figure, the 2X and 4X gear-mesh frequencies are excited. During normal operation, some of the research wind tunnels may be activated and the additional frequencies can be traced to some of these facilities coming on-line. These PSD cascades are the conventional qualitative health monitoring device for the facility.

Figure 10 shows an NSD cascade derived from the digital output of the vibration monitoring system. The smoothing effect of the NSD process is apparent and the relevant frequencies are now indicated by step functions. Quantitative analysis of these data is shown in Figure 11 which depicts the time history of the 10% and 90% energy levels.

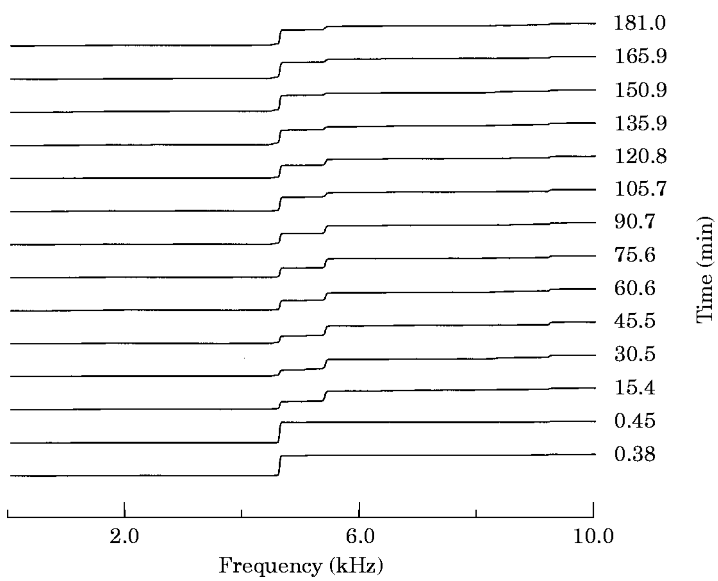

Figure 10. Cascade plot of the normalized spectral distribution derived from the power spectra shown in Figure 9.

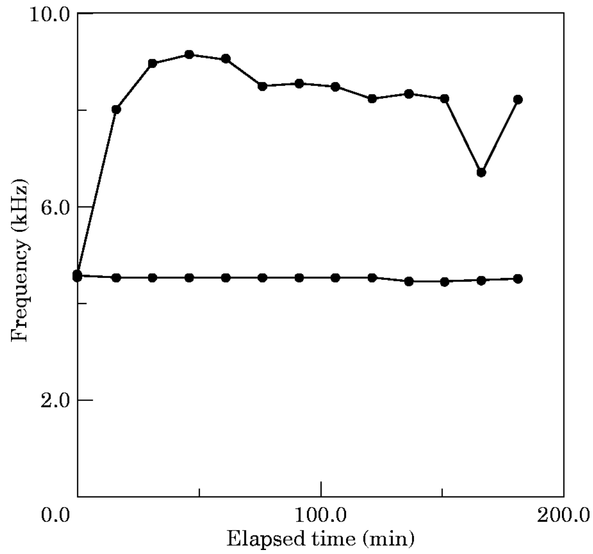

Figure 11. Evolution of the energy at 50% and 90% levels during normal operation of a ground-based compressor.

Initially, all the energy is concentrated at 4600 Hz, as is apparent from both the PSD and NSD. As one or more "events" occur, the energy partition changes and the 90% curve moves to higher frequencies. During the entire test run, the 10% level remains constant since very little energy appears below the 2X frequency. Note the dip in the upper curve just before the end of the run. Detailed examination of the NSD line at 165·9 min show the total relative energy at about 5400 Hz is increased which causes the 90% energy level to drop to a lower frequency relative to its neighbors. Again, it is emphasized that the higher percent energy levels reflect the cumulative contribution to the mean square amplitude rather than only high frequency events. This particular machine is very sensitive to small changes since the signal is dominated by discrete frequencies and the NSD is very flat between the steps. It is expected that machinery with a strong broad band energy spectrum would not be so sensitive.

7. CONCLUSIONS

A procedure based on analysis of the spectral distribution function is described to track specific features of a vibration signal over long time periods. Some advantages of this approach are (1) the SDF is simple to compute as an integration of the PSD. (2) It represents a smoothing operation on the PSD and is not as sensitive to frequency leakage artifacts. (3) The SDF is a monotonically increasing function whose value at any point is the fraction of mean-square energy in the frequency range at and below the indicated value. (4) Contours of time evolving energy partitions are simple features that can be archived for health monitoring purposes. Vibration analysis using the spectral distribution function may have useful application to a wide variety of problems in the new technologies comprising "condition based maintenance."

ACKNOWLEDGMENTS

The author is pleased to acknowledge the efforts of Dave Yaste, Ed Huff, Barry Porter and Manny Irizarry in making the data available. I would also like to thank Jim Laub and Dave Hall for many helpful discussions.

REFERENCES

1. R. J. Hansen, D. L. Hall and S. K. Kurtz 1995 *Transactions of ASME* **117**, 320–325. A new approach to the challenge of machinery prognostics.
2. W. J. Wang and P. D. McFadden 1996 *Journal of Sound and Vibration* **192**, 927–939. Application of wavelets to gearbox vibration signals for fault detection.
3. W. J. Wang and P. D. McFadden 1993 *Mechanical Systems and Signal Processing* **7**, 193–203. Early detection of gear failure by vibration analysis—1. Calculation of the time-frequency distribution.
4. P. J. Diggle 1990 *Time Series*, *A Biostatistical Introduction*. Oxford: Clarendon Press; chapter 4.
5. E. Parzen 1961 *Annals of Mathematical Statistics* **32**, 951–989. An approach to time series analysis.
6. P. M. Batchelder 1967 *An Introduction to Linear Difference Equations*. New York: Dover Publications; chapter 1.
7. V. Wowk 1991 *Machinery Vibration*. New York: McGraw Hill; pp. 149–160.
8. M. L. Hollins 1988 *Detection*, *Diagnosis*, *and Prognosis of Rotating Machinery*. 49–58. The effects of vibration sensor location in detecting gear and bearing defects.